

Organic & Biomolecular Chemistry

Accepted Manuscript



This is an *Accepted Manuscript*, which has been through the Royal Society of Chemistry peer review process and has been accepted for publication.

Accepted Manuscripts are published online shortly after acceptance, before technical editing, formatting and proof reading. Using this free service, authors can make their results available to the community, in citable form, before we publish the edited article. We will replace this *Accepted Manuscript* with the edited and formatted *Advance Article* as soon as it is available.

You can find more information about *Accepted Manuscripts* in the [Information for Authors](#).

Please note that technical editing may introduce minor changes to the text and/or graphics, which may alter content. The journal's standard [Terms & Conditions](#) and the [Ethical guidelines](#) still apply. In no event shall the Royal Society of Chemistry be held responsible for any errors or omissions in this *Accepted Manuscript* or any consequences arising from the use of any information it contains.

1 **Synergism between Genome Sequencing, Tandem Mass**
2 **Spectrometry and Bio-Inspired Synthesis Reveals Insights into**
3 **Nocardioazine B Biogenesis**

4
5
6 Norah Alqahtani^{1, ‡}, Suheel K. Porwal^{1,2 ‡},

7 Elle D. James[¶], Dana M. Bis[¶], Jonathan A. Karty[‡], Amy L. Lane^{*¶},

8 and Rajesh Viswanathan^{*, ‡}

9
10
11
12 ‡ - Department of Chemistry, Case Western Reserve University,
13 Millis Science Center: Rm 216,
14 2074, Adelbert Road, Cleveland OH 44106-7078.

15
16 ¶ - Department of Chemistry, University of North Florida, 1 UNF Drive, Jacksonville, FL 32224.

17
18 ‡ - Mass Spectrometry Facility,
19 Indiana University Department of Chemistry, 800 E. Kirkwood Ave. Bloomington, IN 47405

20 1 Authors contributed equally to this work.

21 2 Present Address: Faculty member, DIT, Univ. of Deharadun, India.

22 * Corresponding authors: Rajesh Viswanathan and Amy L. Lane

23 E-mail: rajesh.viswanathan@case.edu

24 Email: amy.lane@unf.edu

25 **Abstract**

26 Marine actinomycete-derived natural products continue to inspire chemical and biological
27 investigations. Nocardioazines A and B (**3** and **4**), from *Nocardioopsis* sp. CMB-M0232, are
28 structurally unique alkaloids featuring a 2,5-diketopiperazine (DKP) core functionalized with
29 indole C3-prenyl as well as indole C3- and N-methyl groups. The logic of their assembly
30 remains cryptic. Bioinformatics analyses of the *Nocardioopsis* sp. CMB-M0232 draft genome
31 afforded the *noz* cluster, split across two regions of the genome, and encoding putative open
32 reading frames with roles in nocardioazine biosynthesis, including cyclodipeptide synthase
33 (CDPS), prenyltransferase, methyltransferase, and cytochrome P450 homologs. Heterologous
34 expression of a twelve gene contig from the *noz* cluster in *Streptomyces coelicolor* resulted in
35 accumulation of cyclo-L-Trp-L-Trp (**5**). This experimentally connected the *noz* cluster to indole
36 alkaloid natural product biosynthesis. Results from bioinformatics analyses of the *noz* pathway
37 along with challenges in actinomycete genetics prompted us to use asymmetric synthesis and
38 mass spectrometry to determine biosynthetic intermediates in the *noz* pathway. The structures of
39 hypothesized biosynthetic intermediates **5** and **12-17** were firmly established through chemical
40 synthesis. LC-MS and MS-MS comparison of these synthetic compounds with metabolites
41 present in chemical extracts from *Nocardioopsis* sp. CMB-M0232 revealed which of these
42 hypothesized intermediates were relevant in the nocardioazine biosynthetic pathway. This
43 established the early and mid-stages of the biosynthetic pathway, demonstrating that
44 *Nocardioopsis* performs indole C3-methylation prior to indole C3-normal prenylation and indole
45 N1'-methylation in nocardioazine B assembly. *These results highlight the utility of merging*
46 *bioinformatics analyses, asymmetric synthetic approaches, and mass spectrometric metabolite*
47 *profiling in probing natural product biosynthesis.*

48 **Introduction**

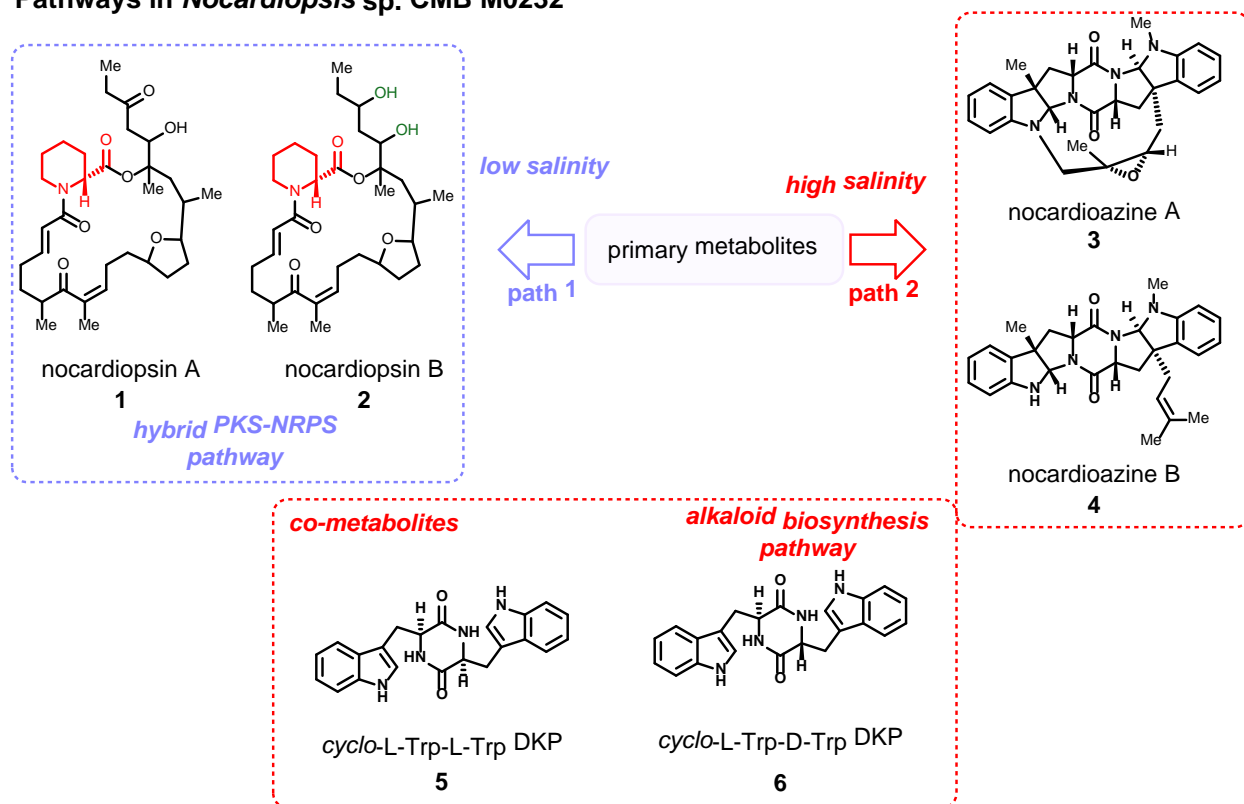
49 Marine actinomycetes continue as rich sources of structurally diverse natural products
50 endowed with promising pharmacological properties.¹ Recently, Capon and co-workers reported
51 isolation and structural characterization of nocardioins² (e. g. **1** and **2**) and diketopiperazine
52 (DKP) containing nocardiozine alkaloids³ (**3-6**) from the marine-derived actinomycete
53 *Nocardioopsis* sp. CMB-M0232 (**Scheme 1**). Intriguingly, under low salinity fermentation
54 conditions, gene regulatory mechanisms predominantly favour biosynthesis of hybrid polyketide
55 and nonribosomal peptide-derived nocardioins, whose biosynthetic pathway we recently
56 established (path 1, **Scheme 1**).⁴ Under relatively high salinity, DKPs including nocardiozines
57 A and B (**3** and **4**), are dominant (path 2, **Scheme 1**).

58 Nocardiozines A and B possess a dimerized tryptophan DKP core. The skeleton
59 comprises seven fused rings (A-B-C-D-C'-B'-A') in a 6-5-5-6-5-5-6 diannulated manner forming
60 a pyrroloindoline-DKP-pyrroloindoline assembly. Among DKP natural products, nocardiozines
61 A and B (**3** and **4**) stand out as the only C3-prenylated DKPs reported from a bacterial source and
62 the first indole-C3-normal prenylated DKP from any source, implicating a unique biosynthetic
63 pathway. The co-isolation of *Cyclo*-L-Trp-L-Trp DKP (**5**) and *Cyclo*-L-Trp-D-Trp DKP (**6**)
64 alongside **3** and **4** alludes to **5** or **6** (or one of their epimers, *Cyclo*-D-Trp-D-Trp DKP, *ent*-**5**) as
65 likely precursors for the more complex congeners **3** and **4**.³ The first reported synthesis of
66 nocardiozine B by Wang et al. corrected the originally assigned stereochemistry of the natural
67 product, alluding to the possibility of *ent*-**5** as a likely intermediate.⁵

68

69 The first enantioselective synthesis of **3** (in addition to other related isoprenylated indole
 70 alkaloids), recently reported by the Reisman group constituted an ingenious strategy towards
 71 synthetically assembling the macrocyclic ring E.⁶ Given the lack of any prior studies on the
 72 characterization of their gene cluster, biosynthetic intermediates and enzymes, the molecular
 73 logic of nocardioazine assembly remains poorly understood. Herein we report the identification
 74 of the *noz* gene cluster encoding nocardioazine B biosynthesis from the draft genome sequence
 75 of *Nocardiosis* sp. CMB-M0232 and characterize pathway intermediates. Our approach of
 76 employing bio-inspired synthetic molecules to elucidate the molecular logic of natural product
 77 assembly represents a relatively overlooked alternative to conventional gene-knockout-guided
 78 approaches. As we demonstrate herein, this strategy is particularly valuable in the many cases
 79 where organisms are not amenable to genetic manipulation.

Pathways in *Nocardiosis* sp. CMB M0232



80

Scheme 1. A. Structures of nocardiosins A (**1**) and B (**2**), nocardioazines A (**3**) and B (**4**), *Cyclo*-L-Trp-L-Trp (**5**) and *Cyclo*-L-Trp-D-Trp (**6**).

81 **Results**82 *Nocardiosis sp. CMB-M0232 draft genome sequence and bioinformatics-based prediction of*
83 *the noz gene cluster*

84 Sequencing and assembly of the *Nocardiosis sp. CMB-M0232* genome yielded a ~6.4
85 Mbp draft with >5500 open reading frames (ORFs) (see SI). The putative *noz* biosynthetic genes
86 are clustered across two separate regions of the *Nocardiosis sp. CMB-M0232* chromosome
87 (**Figure 1**). Bioinformatics analyses of the ORFs revealed candidate enzymes for nocardioazine
88 biosynthesis (**Table 1**). BLASTP analyses of individual predicted ORFs in the entire draft
89 genome revealed both putative nonribosomal peptide synthetases (NRPSs) and a cyclodipeptide
90 synthase (CDPS) as candidates for assembly of the DKP core during the early stage of
91 nocardioazine biosynthesis. However, bioinformatics analyses of adenylation domains from
92 putative NRPSs revealed none predicted to accept two tryptophan substrates.⁷ Further, additional
93 genes clustered with these putative NRPS-encoding genes were strongly suggestive of the
94 biosynthesis of hybrid polyketide synthase -nonribosomal peptide synthase (PKS-NRPS)
95 products⁴ and other classes of secondary metabolites, rather than prenylated diketopiperazine
96 alkaloids. Distinctly, a single putative CDPS (NozA) identified in the draft genome represents
97 the most plausible candidate for assembly of *Cyclo-L-Trp-L-Trp* DKP (**5**) (**Figure 1, Table 1**).

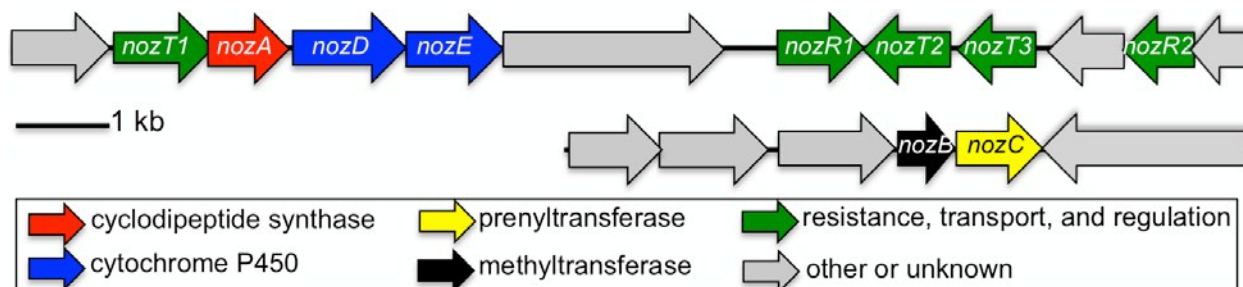


Figure 1. Organization of the two clusters of *Nocardiosis sp. CMB-M0232* biosynthetic genes (*noz*) predicted to play roles in nocardioazine biosynthesis.

<u>Contig #1</u>	# aa	BLASTP annotation	NCBI accession number of homolog	organism	ID / Sim (%)
<i>orf1</i>	421	hypothetical PLP-dependent protein	WP_012786924	<i>Catenulispora acidiphila</i> DSM 44928	51/62
<i>nozT1</i>	402	transporter	AEF16056	<i>Streptomyces vinaceusdrappus</i> NRRL 2363	58/72
<i>nozA</i>	234	cyclodipeptide synthase	YP_003102306	<i>Actinosynnema mirum</i> DSM 43827	35/54
<i>nozD</i>	385	cytochrome P450	KCP45129	<i>Mycobacterium tuberculosis</i> BTB09-382	30/42
<i>nozE</i>	398	cytochrome P450	WP_026248114	<i>Streptomyces</i> sp. MspMP-M5	36/52
<i>orf6</i>	825	adenylosuccinate synthase	WP_016473091	<i>Streptomyces</i> sp. HPH0547	57/70
<i>nozR1</i>	307	XRE family transcriptional regulator	WP_020869817	<i>Streptomyces rapamycinicus</i>	80/89
<i>nozT2</i>	362	ABC transporter	WP_013153583	<i>Nocardiopsis dassonvillei</i>	67/77
<i>nozT3</i>	289	ABC transporter	WP_017566834	<i>Nocardiopsis synnemataformans</i>	76/88
<i>orf10</i>	277	hypothetical protein	WP_018657142	<i>Actinomadura flavalba</i>	59/69
<i>nozR2</i>	136	MerR family transcriptional regulator	WP_017544945	<i>Nocardiopsis prasina</i>	76/84
<i>orf12</i>	216	hypothetical protein	ERT00338	<i>Sporothrix schenckii</i>	36/52
<u>Contig #2</u>	# aa	BLASTP annotation	NCBI accession number of homolog	organism	ID / Sim (%)
<i>orf13</i>	371	hypothetical protein	WP_017620974	<i>Nocardiopsis gilva</i> YIM 90087	73/82
<i>orf14</i>	318	3-ketoacyl-ACP reductase	WP_018724690	<i>Salinispora pacifica</i> CNS055	63/74
<i>orf15</i>	456	family 1 glycosyltransferase	WP_017620972	<i>Nocardiopsis gilva</i> YIM 90087	85/92
<i>nozB</i>	212	indole C3' and N1' methyltransferase	WP_026123683	<i>Nocardiopsis chromatogenes</i> YIM 90109	84/92
<i>nozC</i>	358	indole C3' prenyltransferase	WP_017620970	<i>Nocardiopsis gilva</i> YIM 90087	80/84
<i>orf18</i>	781	hypothetical protein	WP_017625718	<i>Nocardiopsis chromatogenes</i> YIM 90109	68/80

99

100 **Table 1.** Predicted functions of putative nocardioazine biosynthetic enzymes based on
 101 bioinformatics analyses. Two chromosomally distinct gene clusters (contig 1-2) encode these
 102 enzymes. # aa = number of amino acid residues; ID = % identity; Sim = % Similarity.

102

103

104 Analyses of the *Nocardiosis* sp. CMB-M0232 genome revealed a single putative
105 prenyltransferase, NozC (**Table 1**), as the sole candidate for a C3'- normal prenylation of the
106 DKP core. NozC shares homology with enzymes previously annotated as prenyltransferases but
107 for which biosynthetic function has yet to be experimentally confirmed. However, little
108 homology was noted between NozC and biochemically characterized prenyltransferases
109 including the dimethylallyltryptophan synthases FgaPT2⁸ and AnaPT⁹⁻¹⁰. This observation is
110 potentially explained by the unique regioselectivity of NozC as the sole prenyltransferase
111 yielding C3'-normal prenylation. The *nozC* gene is located within a cluster of biosynthetic genes
112 chromosomally distinct from *nozA* (**Figure 1**). The *nozC* prenyltransferase gene is located within
113 the same operon as *nozB*, which encodes a putative methyltransferase that is a candidate for C-
114 and N-methylation of the DKP scaffold. Although the regioselectivity of NozB remains
115 unknown, BLASTP analyses revealed NozB possesses residues conserved among SAM-
116 dependent methyltransferases.¹¹ In **Figure 1** and **Table 1**, all genes predicted by bioinformatic
117 analyses to play enzymatic or regulatory roles in nocardioazine biosynthesis pathway are
118 assigned as "*noz*" genes. Following typical conventions (for annotation of gene clusters), those
119 genes annotated with no apparent role in nocardioazine biogenesis are listed as "orfs" and many
120 of these correspond to hypothetical proteins whose function remain unclear.

121 *NozA is a cyclodipeptide synthase homologous to Amir4627 as revealed through*
122 *bioinformatics*

123 The putative CDPS, NozA, identified by bioinformatics analyses as the most plausible
124 candidate for assembly of *Cyclo*-L-Trp-L-Trp DKP (**5**) was compared with sequences of known
125 characterized CDPSs. Amino acid sequence alignment revealed 35% identity between NozA and
126 Amir_4627, a CDPS from *Actinosynnema mirum* and the only known example of a CDPS

127 incorporating two Trp residues (NCBI Accession #YP_003102306; **Figure 2**).¹² NozA includes
128 residues conserved among related biochemically characterized, catalytically functional CDPSs¹³
129 including Amir_4627¹². Beyond the conserved active site residues (highlighted in yellow),
130 correlations are also apparent between NozA and Amir_4627 for residues implicated in
131 recognition and binding of NozA to aminoacyl-charged tRNA substrates (highlighted brown).
132 Similar predicted secondary and tertiary structural features are noticeable between the two
133 enzymes (Figure 2). Given this prediction, we next sought to establish the connection of the gene
134 cluster harboring *nozA* towards production of cyclo-L-Trp-L-Trp (**5**) through heterologous
135 expression in *S. coelicolor*.
136

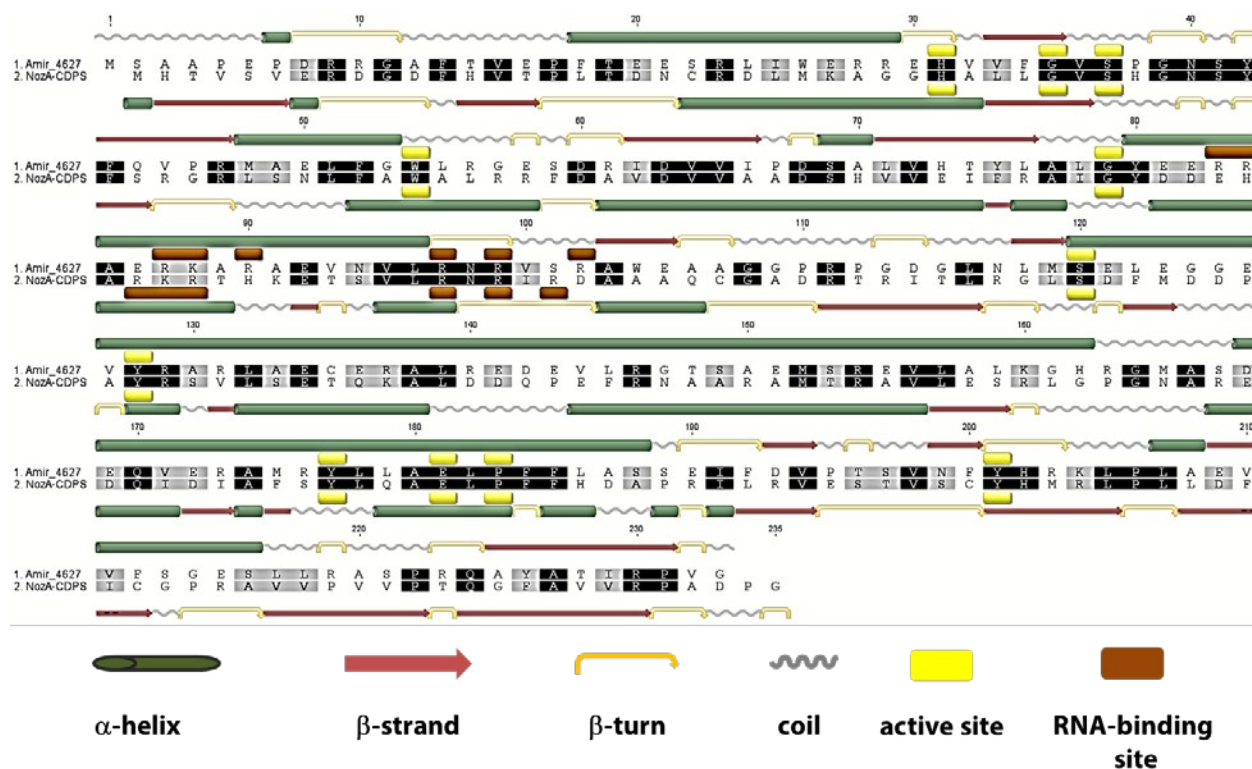


Figure 2. Amino acid sequence alignment between NozA and Amir_4627 and bioinformatics model of NozA generated using GeneiousTM. Clustal ω was used for basic sequence alignment.

137

138

139

140 *Heterologous expression connects contig #1 to Cyclo (L-Trp-L-Trp) biosynthesis*

141 From the SuperCos 1cosmid library generated from genomic DNA, cosmid clone
142 pAL557 was found to carry ~40 kB of the *Nocardiosis* sp. CMB-M0232 genome, including the
143 entirety of contig #1 (**Figure 1, Table 1**). After ensuring that the host organism lacks
144 nocardioazine-like pathway genes, cosmid pAL557 was adapted with genetic elements required
145 for integration into the *Streptomyces* genome and heterologous expression (see SI).¹⁴ This
146 yielded a plasmid (pAL5571), which was introduced by intergeneric conjugation from *E. coli*
147 into *S. coelicolor* M1146, a host engineered for optimized heterologous expression of
148 actinomycete gene clusters.¹⁵ M1146 treatment cultures were fermented in parallel with M1146
149 controls lacking these biosynthetic genes. Metabolite profiles of chemical extracts from these
150 cultures were compared by HPLC with diode array detection, revealing a signal at 11.2 min as
151 the sole discernable metabolite present in treatment cultures and absent from controls (**Figure 3**).
152 The retention time of this metabolite matched that of synthetic *Cyclo*(L-Trp-L-Trp), the
153 generation of which is described below. Further, high-resolution LC/MS supported assignment
154 of the molecular formula of this metabolite as C₂₂H₂₀N₄O₂ (*m/z* 373.1691 [M+H]⁺),
155 corresponding with the formula of *Cyclo*(L-Trp-L-Trp). Based on bioinformatics-predicted
156 functions of proteins encoded by contig #1 (**Figure 1, Table 1**), NozA represents a plausible
157 candidate for catalyzing *Cyclo*(L-Trp-L-Trp) biosynthesis. Ongoing investigations are directed at
158 experimentally establishing the function of NozA.¹⁶

159

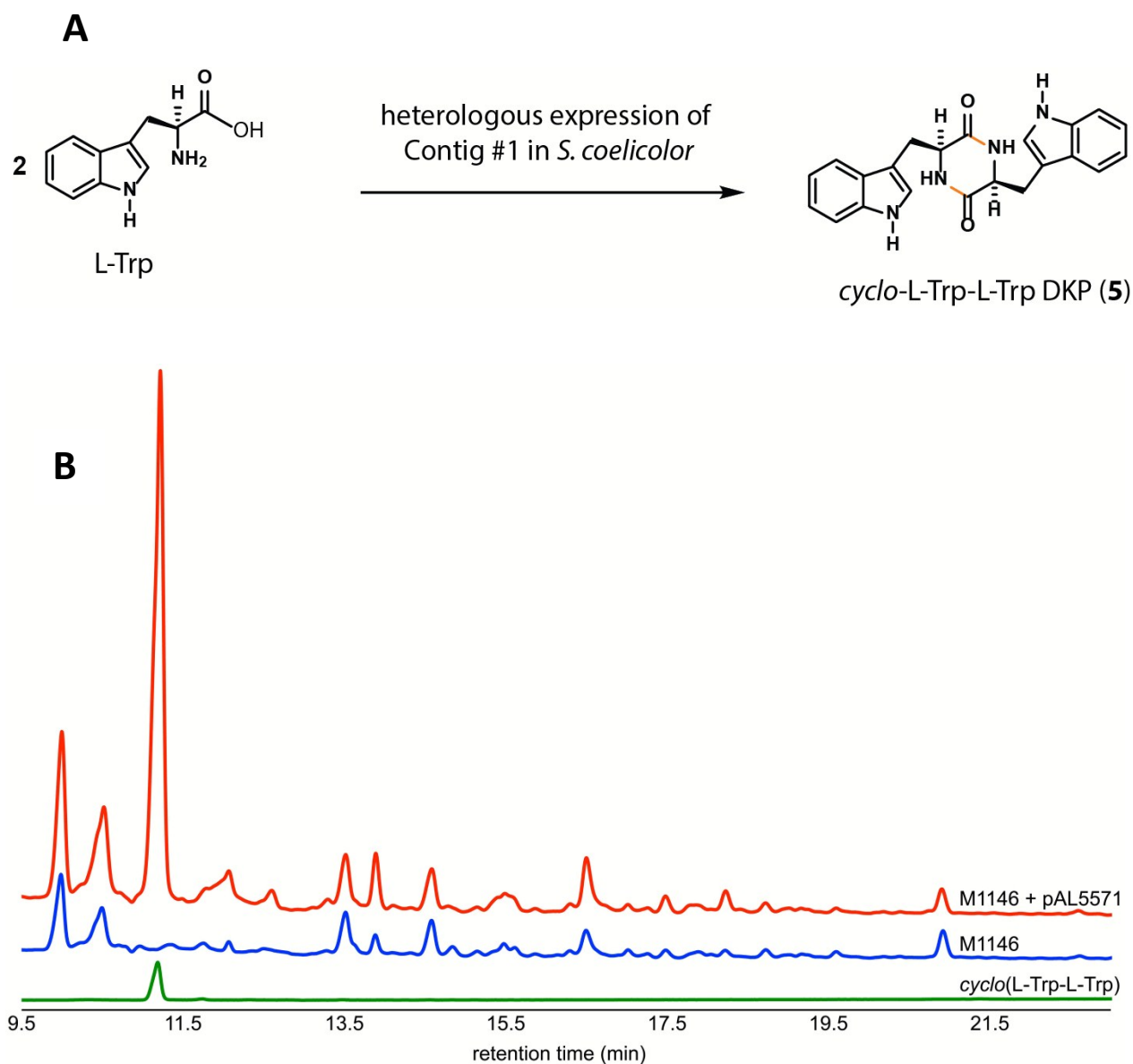


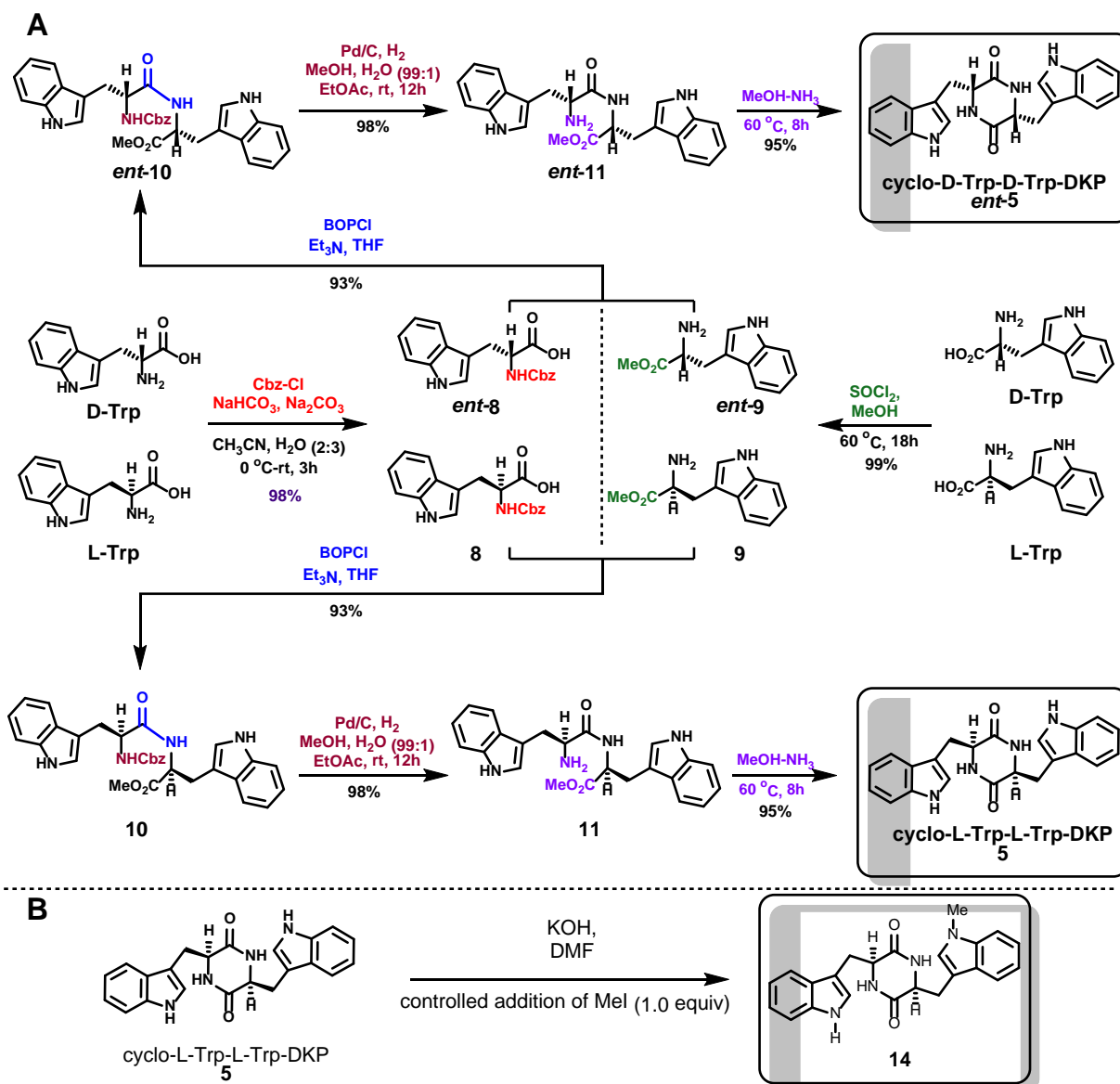
Figure 3. **A.** Formation of *Cyclo*-L-Trp-L-Trp (**5**). **B.** HPLC chemical profiles of *S. coelicolor* M1146 treatment with pAL5571 (shown in red), control M1146 (shown in blue), and *Cyclo*(L-Trp-L-Trp) (**5**) standard (shown in green). UV detection at 280 nm revealed *Cyclo*(L-Trp-L-Trp) (**5**) produced by treatment cultures carrying contig #1 genes but absent from controls lacking these biosynthetic genes. This suggested that NozA catalyzes biosynthesis of this nocardioazine precursor.

161 *Assembly of predicted downstream noz pathway intermediates*

162 Two specific reasons prompted us to turn to synthesis and tandem MS for furthering our
163 knowledge of the *noz* pathway. First, given the recent advancements (in the post-genomics era)
164 in the employment of tandem-MS to connect molecules to individual gene clusters¹⁷, we
165 anticipated assembly of synthetic intermediates may lead to conclusive evidence to support the
166 *noz* pathway. Further, use of tandem-MS-guided strategies can illuminate biosynthetic
167 relationships between multiple pathways encoded by respective gene cluster families.¹⁸ Second,
168 our initial efforts to probe nocardioazine biosynthesis focused on the conventional approach of
169 generating *Nocardioopsis* sp. CMB-M0232 gene replacement mutants with the intention to
170 employ them as tools for determining biosynthetic intermediates. Thus far, *Nocardioopsis* sp. has
171 proven resistant to select gene knockout experiments. Therefore, we turned to the alternative
172 bio-guided synthesis and tandem-MS-centric strategy presented herein to experimentally
173 establish nocardioazine biosynthetic intermediates predicted through bioinformatics analyses.

174 To provide synthetic standards for the *in vitro* characterization of NozA-catalyzed
175 *Cyclo*(L-Trp-L-Trp), and for assembly of downstream pathway intermediates, we constructed **5**
176 and *ent*-**5**. *Cyclo*-(L-Trp-L-Trp) (**5**) was constructed through a four-step sequence, starting with
177 protection of the amino functionality of L-Trp with benzyloxycarbonyl (Cbz) group (**Scheme 2**).
178 Treatment with Cbz-Cl along with sodium bicarbonate-sodium carbonate in acetonitrile-water
179 (2:3; v:v) as solvents, over 3h resulted in **8** providing the western half of the DKP. Similarly,
180 treatment of L-Trp under thionyl chloride in methanol at reflux over 18h resulted in formation of
181 the L-Trp methyl ester (**9**) in near quantitative yield, providing the eastern half of the DKP.
182 BOPCl-mediated coupling of **8** and **9** in the presence of triethylamine as a base in THF resulted
183 in amide **10** in 93% yield. BOPCl-mediated activation of the carboxylic acid functionality of **8**

184 proved the most efficient for isolation of a high yield of amide product **10**. Deprotection of the
185 Cbz group in **10** under hydrogenating conditions in the presence of Pd-C in MeOH (with a trace
186 amount of water) yielded deprotected amine precursor **15** which also contained an ester
187 functionality as an intramolecular reactive partner. The DKP ring system was then formed
188 through the treatment of **11** under 14M ammonia in methanol at 60 °C for 8 h resulting in *Cyclo*-
189 (L-Trp-L-Trp) (**5**) in 95% yield. Likewise, an identical sequence was applied starting from D-Trp
190 (through protection resulting in *ent*-**8** and ester *ent*-**9**, followed by coupling to give *ent*-**10**, finally
191 with deprotection-cyclization step) resulting in the formation of *Cyclo*-(D-Trp-D-Trp) (*ent*-**5**) in
192 excellent overall yield. The four-step sequence was reproduced consistently with identical %
193 yields for either antipode, as shown in **Scheme 2A**. As shown in **Scheme 2B**, we were able to
194 mono-methylate the N1' position of **5** to synthesize **14**.



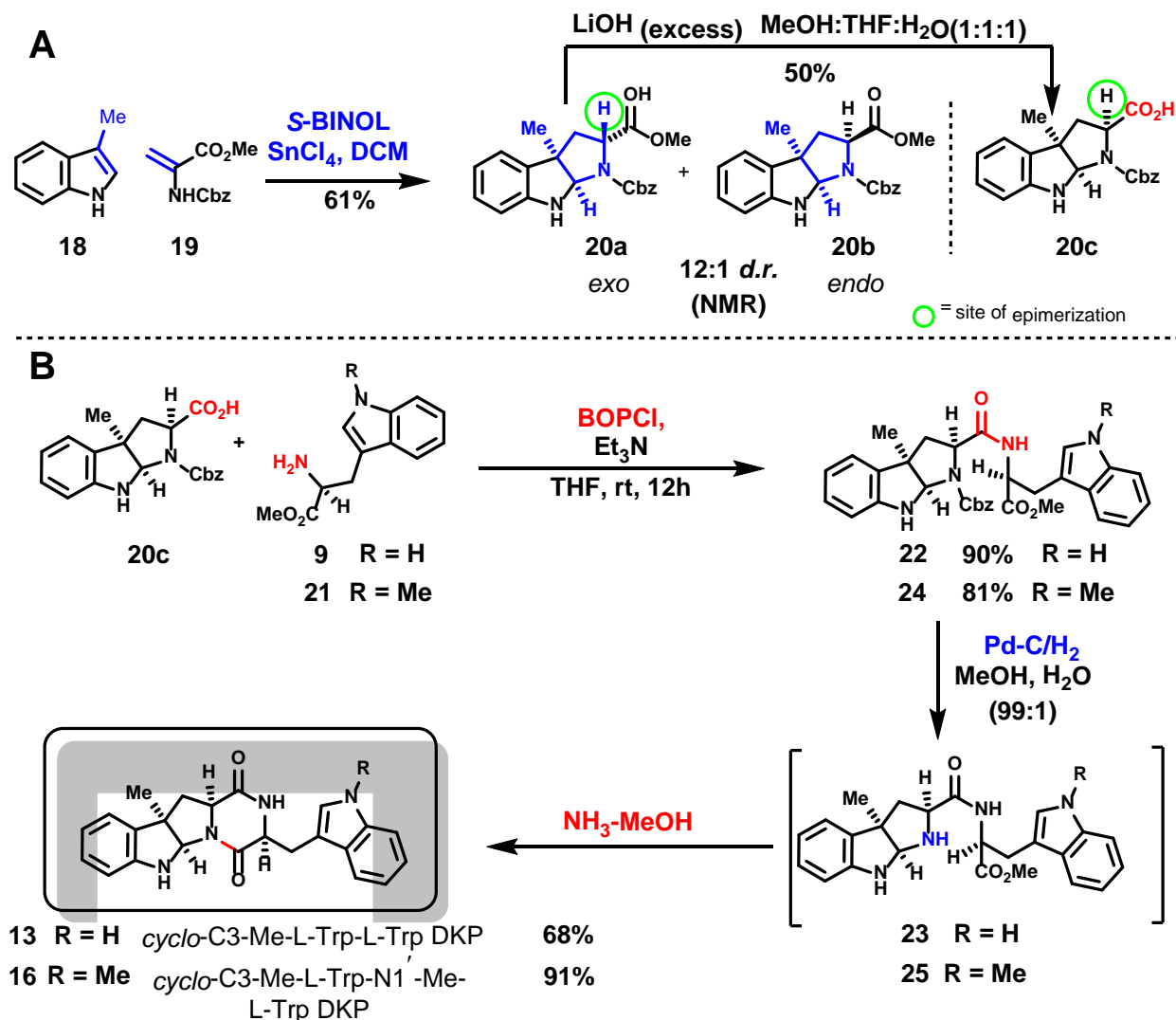
195

196 **Scheme 2. A.** Synthesis of *Cyclo(L-Trp-L-Trp)* (**5**) and *Cyclo(D-Trp-D-Trp)* (*ent-5*). **B.**
 197 Synthesis of N1'-Me-*Cyclo(L-Trp-L-Trp)* (**14**) from **5**. Predicted candidate intermediates of
 198 the *noz* pathway are presented in box.

198

199 Given the bioinformatics-based prediction and homology comparisons of enzymes, we
 200 collectively identified **5**, *ent-5*, **12-17** as candidates for *in vivo* intermediates in the *noz* pathway.
 201 NozB and NozC are expected to catalyze prenylation and methylation steps to yield six unique
 202 potential intermediates (**12-17**) depending on the order of reactions (as described later in **Scheme**

203 5). Additionally, we expected the synthetic endeavour to afford relevant intermediates for future
 204 *in vitro* and *in vivo* reconstitution assays of individual steps catalyzed by NozA, NozB and NozC
 205 in the nocardioazine pathway.



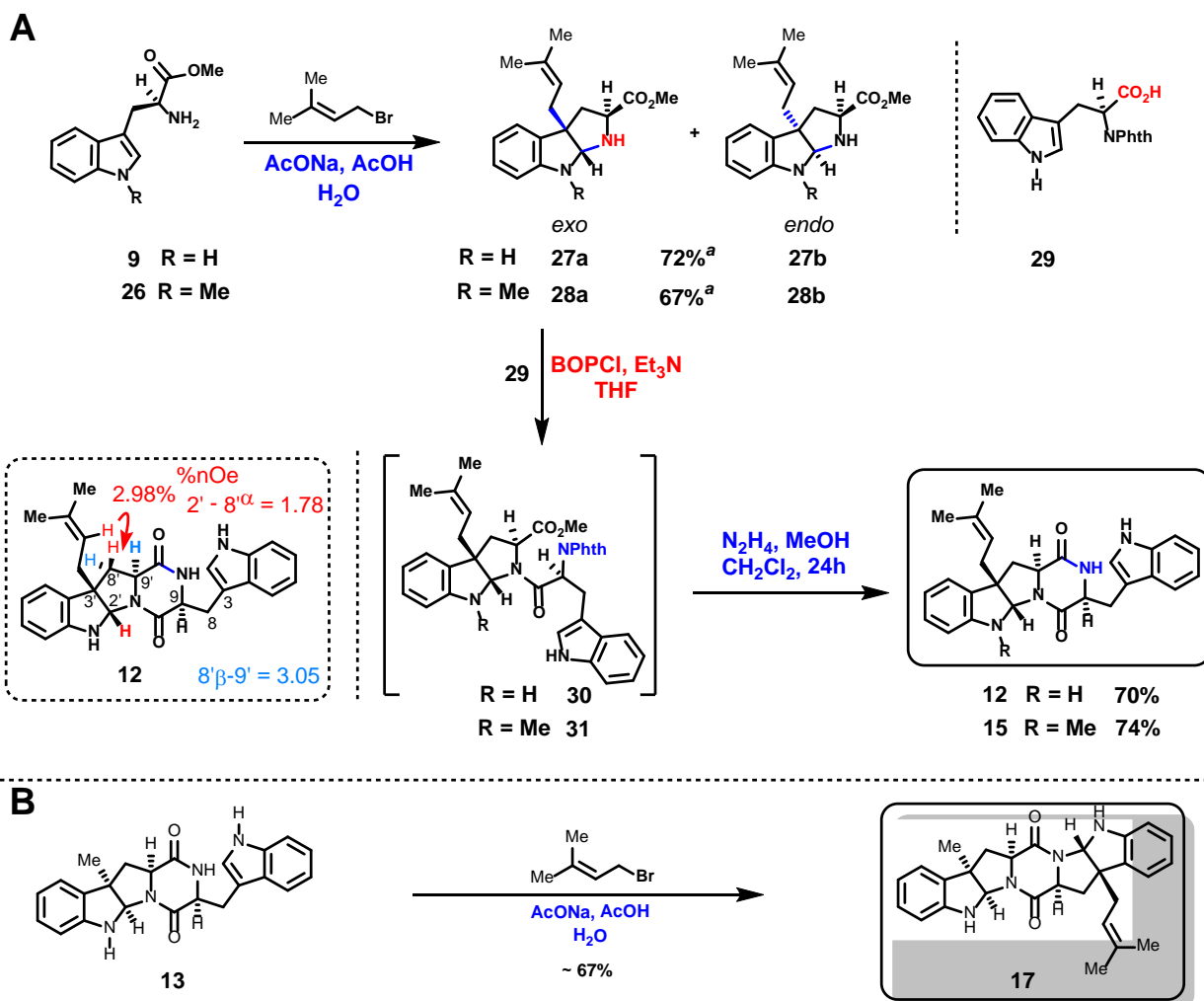
Scheme 3. A. Asymmetric C3-methylation to yield **20**. B. Synthesis of *Cyclo*-C3-Me-L-Trp-L-Trp DKP (**13**) and *Cyclo*-C3-Me-L-Trp-N1'-Me-L-Trp DKP (**16**). Predicted candidate intermediates of the *noz* pathway are presented in box.

209 Due to the relative complexity of the proposed intermediates, regio- and stereoselective
 210 C3'-prenylation, C3-methylation and N1'-methylation presented significant challenges. As
 211 illustrated in **Scheme 3A**, 3-methyl indole (**18**) and enamide (**19**) served as a reasonable starting

212 points to employ an enantio- and diastereoselective indole-enamide [3+2] cycloaddition reaction
213 in the presence of (*S*)-BINOL and tin(IV) chloride as a key step to install the C3-methyl
214 functionality.¹⁹ En route to employing this step as a strategy towards assembling **13** and **16**,
215 enamide **19**, was prepared from L-serine through the conversions involving the corresponding
216 *O*-Boc derivative (see SI). The [3+2] cycloaddition between **18** and **19** proceeded with a 12:1
217 diastereomeric ratio favouring the *exo* isomer **20a** over the minor *endo* isomer **20b**. Each
218 diastereomer exhibited a 2:3 ratio of conformational isomers (caused by the Cbz group on N11
219 position) as revealed by the presence of equivalent sets of ¹H NMR signals. The overall yield of
220 the [3+2] cycloaddition product **20** is 61%. Considering the relative stereochemical disposition
221 of substituents at C2, C3 and C9 in major *exo* isomer **20a**, we initially attempted an LDA-
222 mediated deprotonation-reprotonation sequence to invert the C9 center. By virtue of the lack of
223 an allyl protecting group at N1 (that was present in prior report⁶), a retro-Michael addition
224 occurred, resulting in degradation of **20a** under strongly basic conditions. Therefore, a revision
225 of appropriate conditions to achieve the correct relative stereochemistry was imminent. After
226 careful screening and optimization, treatment with excess lithium hydroxide in a mixture of
227 methanol, water and THF (1:1:1; v:v:v) affected this transformation efficiently to yield **20c**
228 (**Scheme 3A**). Concomitant to the epimerization, we observed base-mediated hydrolysis of the
229 carboxymethyl ester functionality. It proved to be a beneficial outcome as the next step *en route*
230 to **13** involved an amide bond forming coupling to an L-Trp-containing partner **9**. Similar to
231 formation of **10**, we observed smooth peptide bond formation under BOP-Cl-mediated activation
232 of **20c** followed by nucleophilic participation of the amino functionality of **9** resulting in the
233 coupled product **22** in 90% yield in THF as the solvent (**Scheme 3B**). Hydrogenative
234 deprotection of the Cbz group of **22** was affected smoothly to result in **23**. During this

235 deprotection of the Cbz group under Pd-C, we observed direct intramolecular cyclization
236 resulting in formation of **13** in ~10% efficiency. However, this low conversion rate motivated the
237 employment of relatively stronger base²⁰ involving methanolic NH₃ to result in the formation of
238 *Cyclo*-C3-Me-L-Trp-L-Trp DKP (**13**) in high efficiency through the participation of the
239 secondary amino functional group through an internal nucleophilic substitution reaction. The
240 overall synthetic sequence is 5 linear steps starting from 3-methyl indole (**18**). The overall yield
241 for formation **13** was 24.9%. Similarly, the assembly of **16** began with **20a** undergoing a tandem
242 epimerization-hydrolysis event under aqueous lithium hydroxide yielding **20c**. N1'-methylated
243 L-Trp (**21**) was synthesized (from L-Trp, see SI) for its engagement in a coupling step with **20c**.
244 Likewise, **20c** under BOP-Cl activation and triethylamine gave **24** as the product in 81% yield.
245 Similar to the non-methylated counterpart **22**, we could effect a hydrogenative deprotection
246 followed by base-mediated intramolecular cyclization event on **24** to result in **16** (via **25**) in
247 fairly high efficiency (91% yield) in 5 linear steps from commercially available **18**. The overall
248 yield for formation of **16** was 31.0%.

249 As illustrated in **Scheme 4A**, We aimed at *Cyclo*-L-Trp-C3'-*n*prenyl-L-Trp DKP (**12**) and
250 its N1'-methylated variant *Cyclo*-L-Trp-N1'-Me-C3'-*n*prenyl-L-Trp DKP (**15**) as synthetic
251 targets. Through a biomimetic prenylation method we published recently²¹, employment of the
252 methyl ester of L-tryptophan (**9**) served as a precursor to engage in a domino process initiated by
253 a C3'-prenylation event (with prenyl bromide as the electrophile) subsequently resulting in a C-N
254 bond-forming



255
256

Scheme 4. A. Synthesis of *Cyclo*-L-Trp-C3'-*n*-prenyl-L-Trp DKP (**12**) and *Cyclo*-L-Trp-N1'-Me-C3'-*n*-prenyl-L-Trp DKP (**15**). *a* - % isolated yield based on recovered starting material. **B.** Synthesis of *des*-N-Me-Nocardioazine B (**17**). Predicted candidate intermediates of the *noz* pathway are presented in box.

259

260 pyrroloindoline cyclization, under sodium acetate-acetic acid conditions (pH = 2.7) at room

261 temperature, to result in the formation of **27a** and **27b** as a 4:1 mixture of *exo* and *endo*

262 diastereomers. The overall yield for this transformation was 67% considering full recovery of

263 unreacted **9**. The fact that **27a** and **b** were accessed through a single biomimetic step afforded

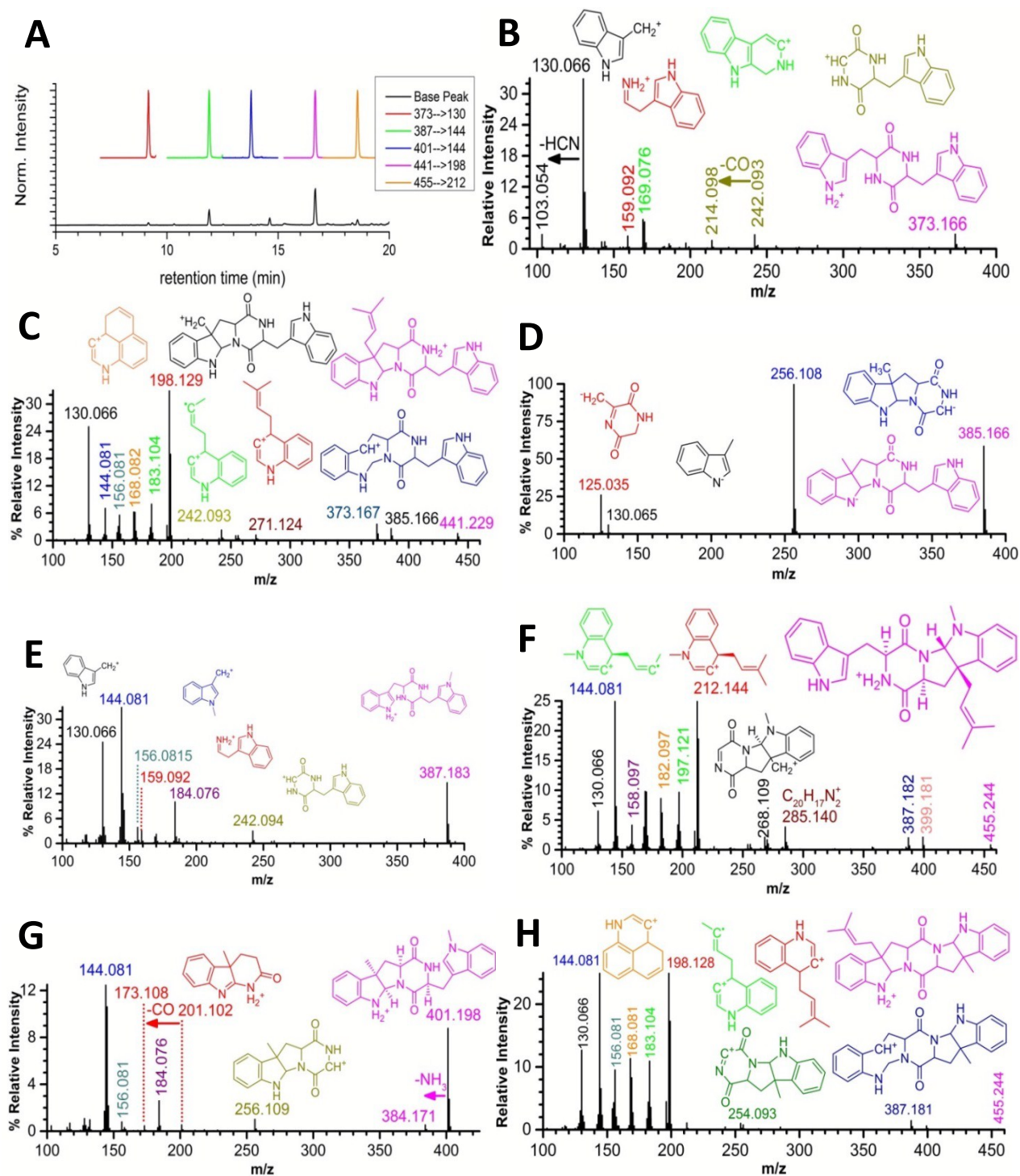
264 direct access to the C3'-normal prenylated scaffold of nocardioazines. Stereochemical

265 relationship between C3'-*n*-prenyl substitution, C2'-H and C9'-carboxymethyl substituent for the

266 major diastereomer **27a** was established through NOESY correlations (see SI). Upon treatment
267 of **27a** with *N*-phthalyl-protected L-Trp-acid **29** (prepared prior using a one-step protection
268 reaction with phthalic anhydride, see SI), under BOP-Cl activation and basic conditions, we
269 obtained the coupled product **30** (comprising the carbon skeleton of target **12**) in 90% yield.
270 Gratifyingly, the coupled product **30** underwent a tandem sequence initiated by a hydrazine
271 hydrate-mediated deprotection of the phthalyl group followed by an intramolecular cyclization in
272 methanol-dichloromethane and resulted in a 70% yield of *Cyclo*-C3'-*n*prenyl-L-Trp-L-Trp DKP
273 (**12**). NOESY experiment showed a 2.98% enhancement between C8'-H and olefinic C2''-H;
274 1.78% enhancement between protons on 2' and 8'- α CH; and finally a 3.05% enhancement
275 between protons on 8' β CH and 9' positions. These confirmed the stereochemistry to be *cis*
276 across the DKP ring system and an overall *exo* arrangement for the B'-C' pyrroloindoline ring
277 fusion. Likewise, engagement of N1'-methylated-L-Trp carboxymethyl ester (**26**) in a one-step
278 prenylation (under aqueous solution) using prenyl bromide resulted in 72% overall yield of C3'-
279 prenylated **28a** (major) and **28b** (minor) based on recovery of unreacted **26**. Similar to the
280 formation of **30**, upon subjecting **28a** to a coupling reaction with **29** using BOP-Cl and
281 triethylamine in THF, we obtained **31** which upon subjecting to a hydrazine hydrate-mediated
282 deprotection-cyclization sequence resulted in the B'-C' ring-forming process leading to *Cyclo*-L-
283 Trp-N1'-Me-C3'-*n*prenyl-L-Trp DKP (**15**) in 74% yield. The overall yields for formation of **12**
284 and **15** were 42.41% and 44.6% over 3 linear steps respectively. *Cyclo*-C3-Me-L-Trp-L-Trp
285 DKP (**13**) underwent C3'-prenylation (similar to prenylations on **9** and **26**) to result in *des*-N1'-
286 Me-Nocardioazine B (**17**). In addition to NMR indicating the presence of a mixture of
287 diastereomers, the identity of **17** for biosynthetic characterization is supported by HPLC (**Figure**
288 **5**), HRMS (**Table 2**) and LC-MSMS (**Figure 4**).

289 *Evaluation of the biosynthetic relevance of synthesized intermediates through NMR, LC-MS*
290 *and HR-tandem MS reveals precursor-product relationships for nocardioazine B biosynthesis*

291 Having synthesized candidate intermediates of the *noz* pathway, we applied LC-coupled-
292 tandem-MS as a tool to establish nocardioazine alkaloidal biosynthetic intermediates. While
293 relatively simpler L-Trp-L-Trp DKP (as products of cyclodipeptide synthase biosynthesis) and
294 other dimeric amino acid DKPs have been analysed through tandem mass spectrometry²²,
295 complex DKPs like **12-17** were thus far not investigated through mass spectrometry adding
296 further importance to this study. EIC traces (**Figure 4A**) indicated that HPLC-MS profiles
297 uniquely separated and distinguished most synthesized intermediates. Unique signatures are
298 observable in MS² spectra for each biosynthetic metabolite (**Figure 4B-H**). Specifically, **Figure**
299 **4B** shows the presence of *Cyclo*-L-Trp-L-Trp DKP (**5**). Its [M+H]⁺ ion (at 373.1662 Da in
300 positive ion mode ESI-MS profile) and its [M-H]⁻ ion (at 371.1530 Da in negative ion mode ESI-
301 MS) are noticeable (see SI). Characteristic Trp fragments were observed as fingerprints of **5**
302 through MS² fragmentation (**Figure 4B**; and Table S2). The product molecular ions, arise out of
303 neutral losses of a Trp moiety (129 Da), along with sequential loss of CO (28 Da) and/or
304 HCONH₂ (45 Da), in various combinations. Neutral loss of HCN (27 Da) from ion at m/z
305 =130.0654 accounted for presence of m/z = 103.0547 ion. Likewise, we mapped tandem MS
306 signatures of *Cyclo*-L-Trp-C3'-*n*-prenyl-L-Trp DKP (**12**); *Cyclo*-C3-Me-L-Trp-L-Trp DKP (**13**);
307 *Cyclo*-N1'-Me-L-Trp-L-Trp DKP (**14**); *Cyclo*-L-Trp-C3'-*n*-prenyl-N1'-Me-L-Trp DKP (**15**);
308 *Cyclo*-C3-Me-L-Trp-N1'-Me-L-Trp DKP (**16**) and *des*-N1'-Me Nocardioazine B (**17**), as
309 illustrated in **Figure 4** (additionally in SI).



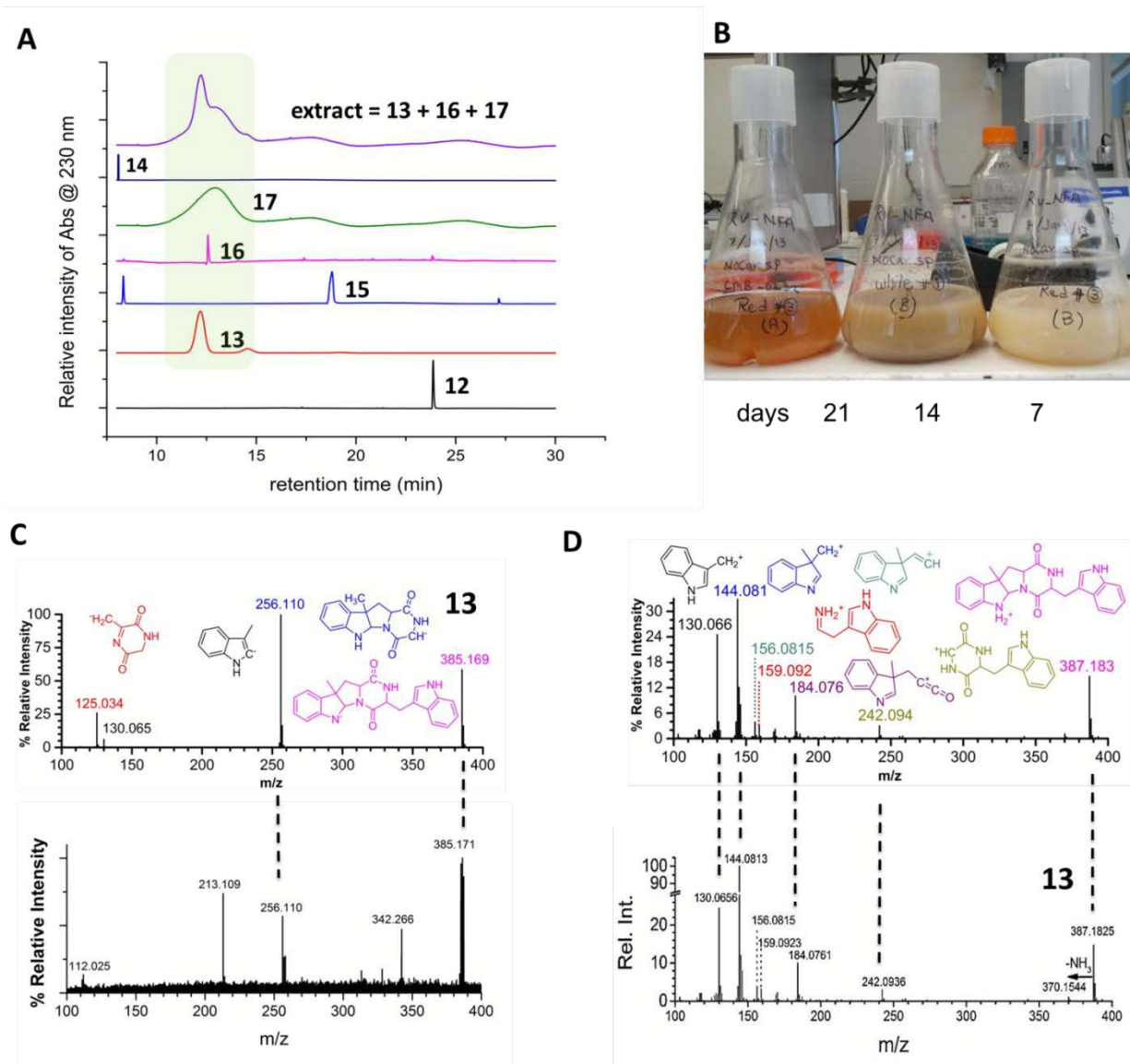
310

Figure 4. A. Extracted ion chromatograms (EICs) traces of synthetic standards. ESI TOF-MS² fragmentation data: B. *Cyclo-L-Trp-L-Trp* DKP (**5**) ($M+H$)⁺; C. *Cyclo-L-Trp-C3'-prenyl-L-Trp* DKP (**12**) ($M+H$)⁺; D. *Cyclo-C3-Me-L-Trp-L-Trp* DKP (**13**) ($M-H$); E. *Cyclo-N1'-Me-L-Trp-L-Trp* DKP (**14**) ($M+H$)⁺; F. *Cyclo-L-Trp-N1'-Me-C3'-prenyl-L-Trp* DKP (**15**) ($M+H$)⁺; G. *Cyclo-C3-Me-L-Trp-N1'-Me-L-Trp* DKP (**16**) and H. *des-N1'-Me nocardioazine B* (**17**).

311 Next, we looked for signatures of **12-17** directly from cultures of *Nocardiosis* sp. CMB-
312 M0232 to detect their presence as biosynthetic intermediates *in vivo*. Reverse-phase HPLC
313 uniquely identified synthetic **12-16** (**Figure 5A**). Comparison of retention times of these
314 synthetic compounds with the alkaloidal fractions of *Nocardiosis* sp. CMB-M0232 revealed
315 that **12**, **14** and **15** were not relevant biosynthetic products or intermediates. Interestingly, we
316 detected the presence of three relevant metabolites in *Nocardiosis* sp. extracts, namely, **13**, **16**
317 and **17**. Further supporting its biosynthetic relevance, TLC patterns of extracts showed presence
318 of **13** (see Figure S11). We compared the MS² fragmentation pattern of **13** extracted from the
319 bacterial culture to that of the synthetic standard. The ESI-TOF-MSMS data for synthesized **13**
320 overlapped precisely with that of the extracted metabolite (**Figure 5C and D**). The ion at m/z =
321 256.110 (C3-methyl group containing Trp-DKP) from the m/z 385.2 precursor ion after loss of a
322 neutral Trp unit (129 Da) was observed both in the synthesized standard as well as from the
323 extract. Further, ¹H and ¹³C NMR analyses (of LC-derived extracts) confirmed the structure of
324 this metabolite as **13** (Figure S12 and S13, SI). Despite modifying several solvent conditions and
325 flow rates, we were unable to distinctly separate **17** out of overlap in retention time from **13** and
326 **16**. Overall, this approach of combining synthesis, LC and tandem MS gave a global picture of
327 the biosynthetic map for the *noz* pathway. The map in **Scheme 5** was derived from LC-MS²
328 investigations for all of the intermediates. An intermediate was considered “observed” if its
329 retention time and MS² pattern seen in bacterial extracts matched those of the synthetic standard.

330

331



332

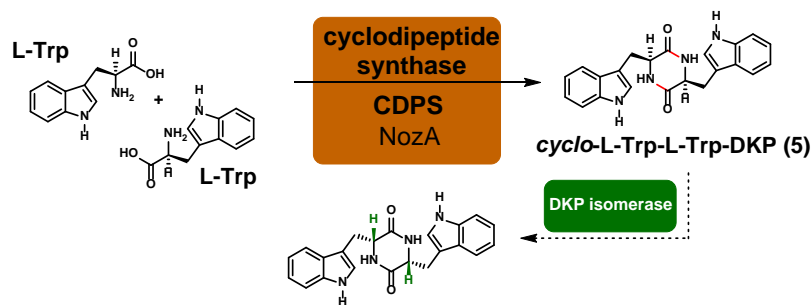
333

Figure 5. **A.** Reverse phase HPLC traces for synthesized and extracted metabolites from *Nocardioopsis* sp. CMB-M0232. **B.** Culture of *Nocardioopsis* sp. CMB-M0232 at 7, 14 and 21 days. **C.** ESI(-)-TOF-MSMS spectrum of **13** from *Nocardioopsis* sp. CMB-M0232 (top) matched with spectrum of synthesized **13** (bottom); **D.** ESI(+)-TOF-MSMS spectrum of **13** from *Nocardioopsis* sp. CMB-M0232 (top) matched with spectrum of synthesized **13** (bottom).

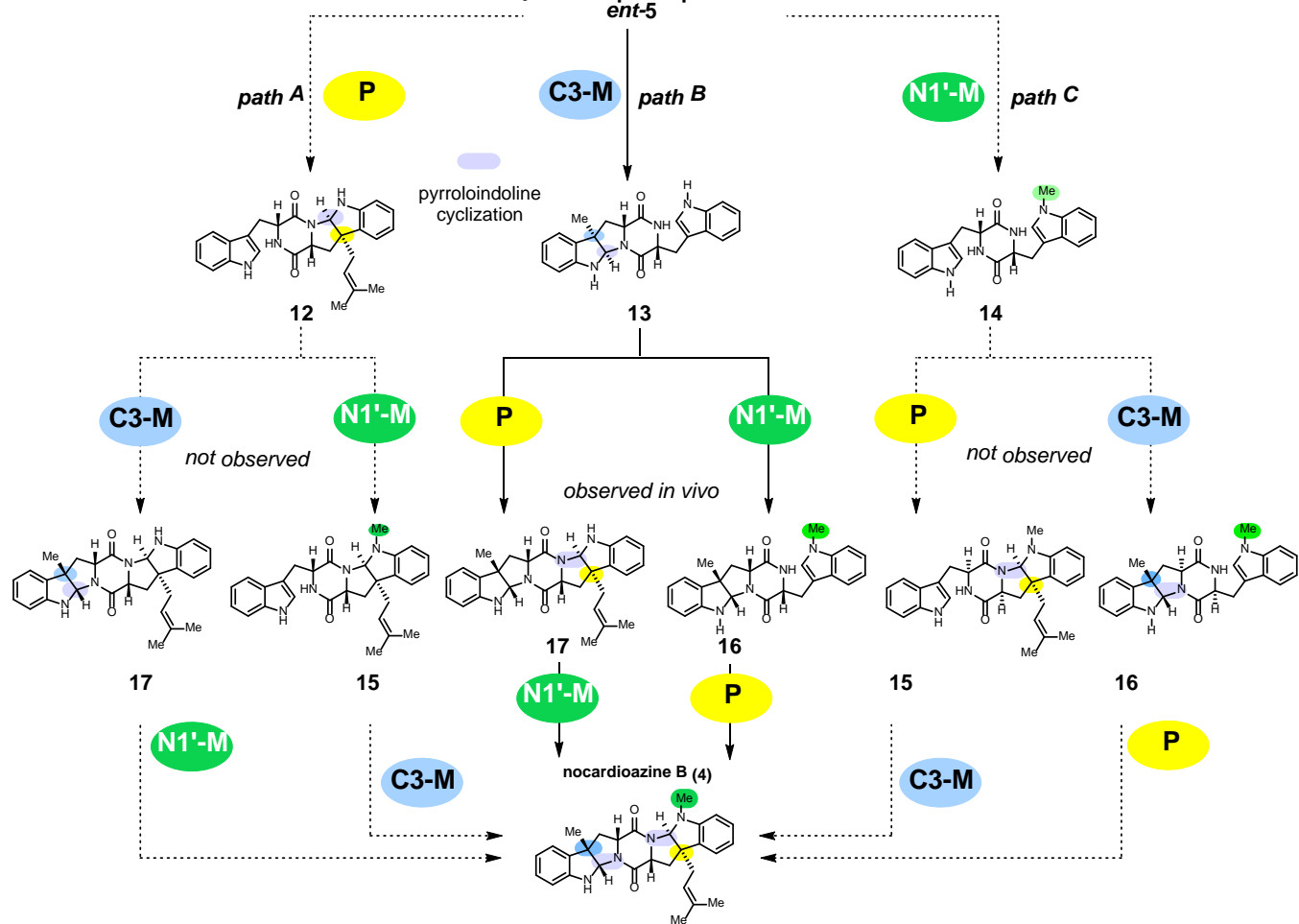
Name of Metabolite	Molecular Formula	ESI HR-MS [M] ⁺ [M+H] ⁺ [M-H] ⁻ (expected) Found	LC retention time Found (synth.) (min)	MS ² Fragmentation Pattern	Biosynthetic Role	Observations
<i>Cyclo</i> -L-Trp-L-Trp DKP (5) and <i>Cyclo</i> -D-Trp-D-Trp DKP (<i>ent</i> - 5)	C ₂₂ H ₂₀ N ₄ O ₂	(372.1586) (373.1659) (371.1513) 373.1665 (+) and 371.1530 (-)	7.06 (7.06)	242.0925; 144.0805 and 130.0654	early stage intermediate	[M+H] ⁺ and [M-H] ⁻ observed in extracts Matches with synthetic standard
<i>Cyclo</i> -L-Trp-C3'-prenyl-L-Trp DKP (12)	C ₂₇ H ₂₈ N ₄ O ₂	(440.2212) (441.2285) (439.2139) NF	NF (23.2)	373.1671; 242.0931; 113.0337; 198.1288; 183.1044; 130.0658	Mid stage product of C3'-prenyltransfer on 5	Not detected
<i>Cyclo</i> -C3-Me-L-Trp-L-Trp DKP (13)	C ₂₃ H ₂₂ N ₄ O ₂	(386.1743) (387.1816) (385.1670) 387.1825 385.1711	11.8 (11.8)	385.1690; 256.110; 130.065	Mid stage product of C3-methyltransfer on 5	[M+H] ⁺ and [M-H] ⁻ observed in extracts Matches with synthetic standard
<i>Cyclo</i> -N1'-Me-L-Trp-L-Trp DKP (14)	C ₂₃ H ₂₂ N ₄ O ₂	(386.1743) (387.1816) (385.1670) 387.1825 385.1711	NF (9.5)	242.0932, 184.0761, 144.0814	Mid stage product of N1'M methyltransfer on 5	Not detected
<i>cyclo</i> -L-Trp-N1'-Me-C3'-prenyl-L-Trp DKP (15)	C ₂₈ H ₃₀ N ₄ O ₂	(454.2369) (455.2442) (453.2296) NF	NF (18.0)	399.1806; 212.1441; 144.0813; 130.0657	mid stage product of indole N1' methyltransfer on 12	Not detected
<i>Cyclo</i> -C3-Me-L-Trp-N1'-Me-L-Trp DKP (16)	C ₂₄ H ₂₄ N ₄ O ₂	(400.1899) (401.1972) (399.1826) 401.1972	12.2 (12.2)	401.1981, 256.1089, 184.0761, 144.0813	Mid stage indole N1'-methyltransferase product from 13	[M+H] ⁺ observed in extracts Matches with synthetic standard
Des-N1'-Me-nocardioazaine B (17)	C ₂₈ H ₃₀ N ₄ O ₂	(454.2369) (455.2442) 455.2442	12.6 (12.6)	256.1089; 184.0761; 144.0813	Putative precursor to secondary metabolite product 4	[M+H] ⁺ observed in extracts
Nocardioazaine B (4)	C ₂₉ H ₃₂ N ₄ O ₂	(468.2525) (469.2598) 469.2695	18.44*	186.0914 156.0812 144.0805 and 130.0654	Putative precursor to secondary metabolite product 3	[M+H] ⁺ observed in extracts
Nocardioazaine A (3)	C ₂₉ H ₃₀ N ₄ O ₃	(482.2318) (483.2396) (481.224) 483.2396	8.80*	483.2396	Secondary metabolite product	[M+H] ⁺ observed in extracts

334 **Table 2.** LC-MS and MSMS data for synthetic and extracted biosynthetic intermediates and products. **NF** –
 335 not found; for full detailed listing and corresponding formulas of molecular ions, see SI. Note: metabolites
 with Mw = 369, 383, 482, 466, 468 and 452 were identified as DKPs in Capon's study.^{2, 4} Ions represented
 in **bold** are identified from extracts of *Nocardopsis* sp. CMB-M0232. * - No synthetic standard, exact mass
 match only. Shaded entries represent those metabolites experimentally observed in *Nocardopsis* extracts.

A early stage



B mid stage



336

Scheme 5. Biosynthetic steps for early- and mid-stages of *noz* pathway. Dotted lines show hypothesized possibilities and bold lines show the path that is evident from HPLC, LC-MS, MSⁿ analyses for all relevant intermediates.

337

338 Upon consideration of the three mid-stage enzymatic steps in a simple permutation
339 fashion (**Scheme 5**), the multi-pronged approach reveals the relevance of *C3-methylation as a*
340 *step preceding C3'-prenylation and N1'-methylation*. Specifically, if *Nocardioopsis* sp. CMB-
341 M0232 were to employ an indole C3'-prenyltransferase (hypothetical NozC) to install a dimethyl
342 allyl group on DKP **5** then the product of this biosynthetic reaction is expected to be *Cyclo-L-*
343 *Trp-C3'-prenyl-L-Trp* DKP (**12**). The formation of pyrroloindoline cycle (of **12**) during this
344 prenyltransfer step is based on fungal precedents such as FgaPT2.⁹ Alternatively, if the indole
345 C3-methyl transferase (NozB) were operative on the basic early-stage intermediate DKP **5**, the
346 product expected out of this transformation is represented by *Cyclo-C3-Me-L-Trp-L-Trp* DKP
347 (**13**). The corresponding N1'-methylated product from action of a methyltransferase (NozB, but
348 regioselectively on the N1' position) would be *Cyclo-L-Trp-N1'-Me-L-Trp* DKP (**14**). Products
349 **15**, **16** and **17** represent further increase of complexity through a subsequent enzymatic event.
350 Their relevance in a combinatorial way is discussed in **Scheme 5**. N1'-methylation of **13** will
351 lead to production of **16** and therefore we anticipated the presence of **16** from cultured
352 *Nocardioopsis* sp. CMB-M0232. Indeed, LC-ESI-(+)TOF MSMS analysis indicated the presence
353 of **16** at $R_t = 12.2$ min (Figure S6 in SI). HRMS verification of its presence was confirmed
354 through observation of an ion at $m/z = 401.1972$ and furthermore, MS² fragmentation revealed
355 presence of characteristic ions at $m/z = 256.109$, 184.076 , and 144.081 that matched well with
356 synthesized **16** (**Table 2**). Presence of des-N1'-Me nocardioazine B (**17**) was detected through
357 the identification of a broad LC peak at $R_t \sim 12.6$ min that corresponded to an HR-MS signal at
358 $m/z = 455.2442$ ($\Delta m = 0$ ppm). Its corresponding MS² spectra revealed signature peaks at m/z
359 256.1089 (seen in fragmentation of **13**+14 Da), 184.0761 , and 144.0813 typically observed for
360 all synthetic standards possessing the C3-methyl substitution and two Trp units of the DKP ring

361 system (**Table 2**). Significantly **12**, **14** and **15** were *not* identified from cultures of *Nocardioopsis*
362 sp. CMB-M0232 as verified through the conspicuous absence of signature prenylated ions at m/z
363 = 198.129 ($C_{14}H_{16}N^+$) *observed only in 12* and a corresponding ion *seen only for 15* at m/z =
364 212.144 ($C_{15}H_{18}N^+$). Pathway specific metabolites identified through LC and their MS-MS
365 fragmentation (in this study) are highlighted green in **Table 2**.

366 Discussion

367 Synergistic Approach Establishes Pathway to Nocardioazine B

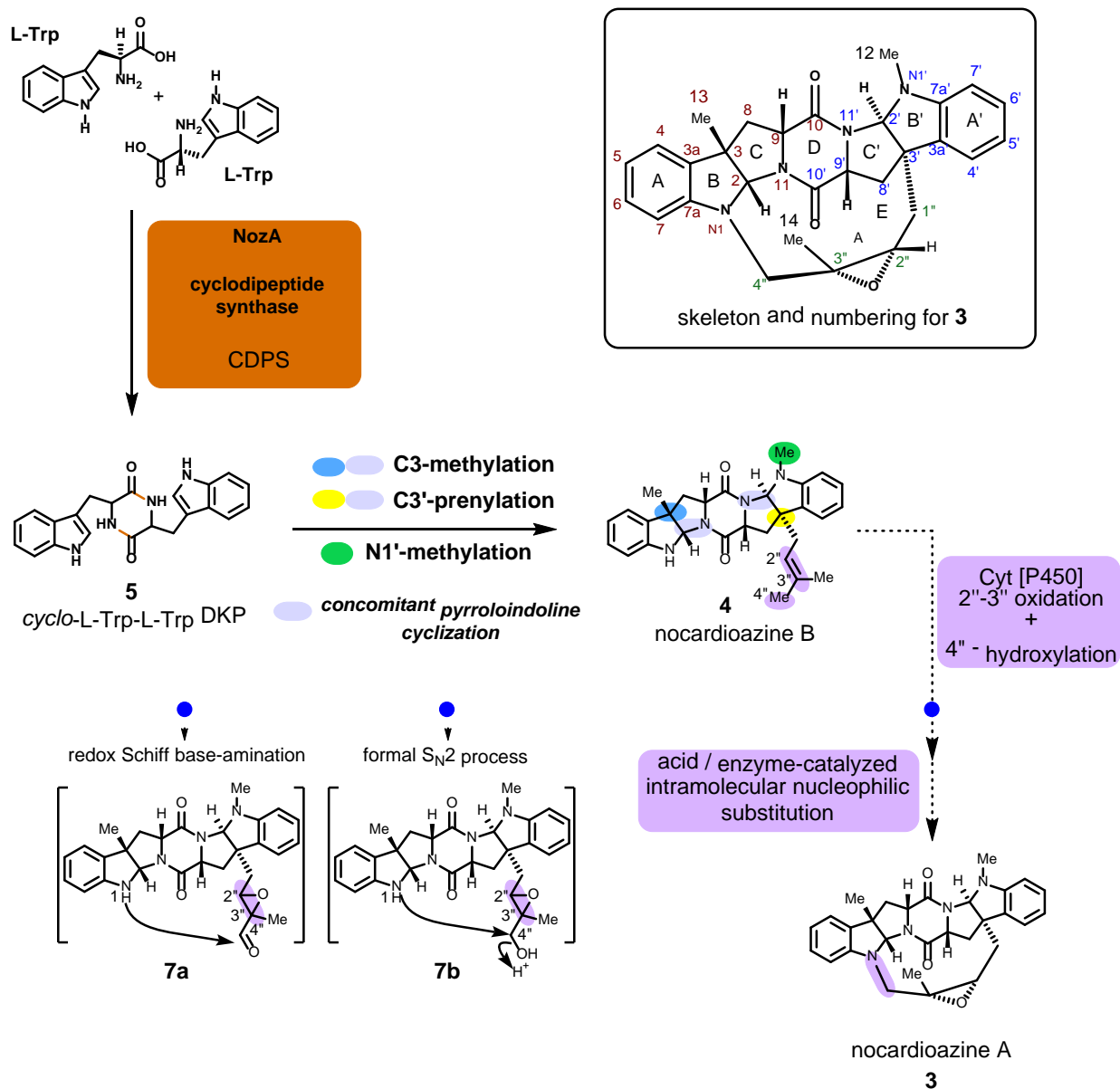
368 Microbial systems continue to inspire discovery of novel biocatalysts for the synthesis
369 organic molecules with unique structural and biological properties.²³ We present evidence that
370 points to early stage assembly of *Cyclo*-Trp-Trp DKP as an intermediate that undergoes a regio
371 and stereoselective C3-methyltransfer step resulting in the formation of a subsequent
372 intermediate that is C3-normal prenylated and N1'-methylated by respective enzymes encoded
373 in the *noz* pathway with reasonable promiscuity in the order of their occurrence. These results
374 illuminate the specific precursor-product relationships in the nocardioazine alkaloid biosynthetic
375 pathway and are expected to guide future genetic and enzymatic studies to further probe the *noz*
376 pathway. The latent symmetry present in the DKP ring system of **3** and **4** enables numbering
377 (N1-N11 and N1'-N11') of the skeletal constituents comprising the 6-5-5-6-5-5-6 skeleton that
378 includes rings A-B-C-D-C'-B'-A' respectively (**Scheme 6**). Nature has further decorated the
379 western half of the DKP core through a methyltransferase-catalyzed regio- and stereoselective
380 indole C3-methylation event resulting in the pyrroloindoline B-C ring fusion. The fungal
381 prenyltransferase enzymology offers a precedent for pyrroloindoline formation through
382 enzymatic functionalization of the indole-C3 position accompanied by a concomitant cyclization
383 event between N11 and C2 positions.⁹ The B'-C' rings, on the eastern side of the DKP core, are

384 functionalized through a prenyltransferase-catalyzed regio- and stereoselective indole C3'-
385 normal prenylation event (with a 3'-1'' head-to-head connectivity) and a concomitant N11'-C2'
386 bond-forming cyclization generating des-N1'-Me-nocardioazine B (**4**). Further, indole N1'-
387 methylation (at C12) is observed as a likely event catalyzed by an N-methyltransferase leading to
388 **3** and **4**. Overall, these three pivotal biosynthetic events create the asymmetry in the two
389 annulated pyrroloindoline moieties of **3** and **4**. The mid-stages of the pathway offered a
390 reasonably sized cohort of synthetically tractable intermediates that could be used as standards
391 for HPLC and LC-MS² analyses. These experiments facilitated identification of the order of
392 biosynthesis *in vivo*.

393 Thus far, bioinformatics analyses by previous researchers have predicted more than 50
394 gene clusters to encode CDPS machinery for assembly of DKP natural products in various
395 species spanning both prokaryotes and eukaryotes.²⁴ However, far fewer of these CDPSs have
396 been biochemically characterized.^{12-13,25-26} Only a single experimentally characterized CDPS,
397 Amir_4627 from *Actinosynnema mirum* has been established to yield *Cyclo*-L-Trp-L-Trp DKP
398 as the dominant product.¹² Homologs of NozA are evident in a range of *Nocardioopsis* strains
399 whose CDPS-containing gene clusters are available in publically deposited genomes. For
400 example, *Nocardioopsis alba* encodes an enzyme (AlbC) possessing 40% sequence identity to
401 NozA.²⁵ To date, biochemically characterized CDPSs have been reported to catalyze the
402 formation of DKPs exclusively from L-amino acids. This is due to the mechanism of CDPSs,
403 which employ aminoacyl-charged tRNAs from primary metabolism as substrates in catalyzing
404 formation of the DKP scaffold. Hence, if nocardioazines A-B (**3-4**), featuring D-amino acid
405 stereochemistry, are indeed CDPS-derived, then an unidentified isomerase is also expected as a

406 required component of their biosynthetic pathway to isomerize *Cyclo*-L-Trp-L-Trp DKP (**5**) into
 407 its antipode *ent*-**5**.

Biosynthetic Steps to **3**



Scheme 6. Steps in the *noz*-encoded pathway illustrated as a function of known and unknown stages. Nocardiozine numbering is illustrated in box.

410 As illustrated in **Scheme 5**, it is evident that the methyltransferase step, likely
411 encoded by **NozB**, in *Nocardioopsis* sp. CMB-M0232 is successively processing methylations
412 of **5** and **13**. The possibility of the recruitment of a promiscuous indole C3'-normal
413 prenyltransferase that could prenylate either **13** or **16** leading to **17** or **4** is plausible.
414 Nocardioazine A (**3**) has an additional isoprenoid-tethered DKP scaffold comprised of an 11-
415 membered macrocycle (ring E) bridged between N1 and C3' (tether numbered as 4''-3''-2''-1'').
416 P-glycoprotein-mediated efflux pump (P-gp) inhibition is exhibited specifically by **3**, by virtue of
417 the macrocycle E.³ The biosynthetic pathway to nocardioazine A probably incorporates **4** as a
418 reasonable intermediate, and employs a few additional oxidative transformations in tethering two
419 annulated pyrroloindoline rings with a 5-carbon isoprenoid moiety. Cytochrome P450
420 homologs²⁷ NozD and NozE (**Figure 1**, **Table 1**) represent candidates for oxidative
421 transformation of **3** to afford **4**. According to Raju et al.³, the C2''-C3'' olefinic bond is mono-
422 oxidized into an oxirane and the C4'' position participates in an intramolecular cyclization event
423 with the indolic nitrogen of the B-ring on **7** to close the macrocycle. Two possible intermediates
424 (**7A** or **B**) for this late stage of the pathway is presented in **Scheme 6**. 2,5-Diketopiperazines of
425 α -amino acids are valuable structural cores that have inspired natural products research.²⁸ Bio-
426 inspired synthesis complementing genetic studies of such a privileged core, as detailed herein,
427 therefore has potential to allow new synthetic pathways towards creation of structural analogs
428 through chemo enzymatic pathways and mutasynthesis.

429 Conclusion

430 Nocardioazines A and B (**3** and **4**), as the first indole-C3-normal prenylated DKPs from
431 any biological source, present a poorly understood pathway. In this study, we laid the chemical
432 foundations of nocardioazine biosynthesis by synthesizing an exhaustive set of putative,

433 bioinformatics-predicted intermediates. Structural verification through 1D and 2D NMR, and
434 analyses through HPLC-MSMS and HRMS methods established the framework for evaluation of
435 the biological relevance of specific intermediates in the proposed *noz* (nocardioazine) pathway *in*
436 *vivo*. Upon comparing HPLC and tandem mass spectrometry data between synthesized standards
437 and alkaloidal fractions extracted from *Nocardioopsis* sp. CMB-M0232, it is conclusively evident
438 that indole C3-methylation leading to **13** is a biosynthetic event that precedes indole C3'-normal
439 prenylation and a second methyl transfer to the N1' position. In addition, through bioinformatics
440 analyses of the draft genome of *Nocardioopsis* sp. CMB-M0232, heterologous expression of
441 Contig #1 was shown to result in the assembly of *Cyclo*-L-Trp-L-Trp (**5**) as a precursor to the
442 nocardioazine alkaloids. Future efforts are necessary to unveil the complete genetic and
443 enzymatic-underpinning of nocardioazine A and B biosynthesis. Collectively, these results
444 highlight the utility of synergizing bioinformatics analyses, asymmetric synthesis, and mass
445 spectrometric metabolite profiling in guiding natural product biosynthesis studies.

446 **Acknowledgements**

447 We gratefully thank Prof. Robert J. Capon (University of Queensland, Australia) for
448 providing *Nocardioopsis* sp. CMB-M0232 isolate. We are grateful to Drs. Mervyn J. Bibb and
449 Juan Pablo Gomez-Escribano for providing *S. coelicolor* M1146. RV, NFA and SKP thank Case
450 Western Reserve University's Department of Chemistry for funding portions of this project. NFA
451 thanks the Saudi Arabian Ministry of Higher Education for graduate financial aid. Saudi Arabian
452 Cultural Mission (SACM) and Drs. Rashed M. Alsedran (Director) and Elbreir Mohammed
453 (academic Advisor) are thanked by NFA for academic support. Authors thank Dr. Dale Ray for
454 expert NMR data collection. Authors thank Dr. Ormond Brathwaite for technical support for
455 culturing *Nocardioopsis* sp. CMB-M0232 strain for metabolic extraction. We thank Prof. Robert

456 Salomon and Dr. Mikhail Linetsky for expert technical support. Authors thank Angela Hansen
457 and Taylor Harmon for support with collection of mass spectrometry data. Authors thank
458 William Frank of SIRC (CWRU) for instrumentation support. ALL is grateful for funding from
459 a Research Corporation Cottrell College Science Award, a UNF Transformational Learning
460 Opportunity Award, and a UNF Academic Affairs Scholarship grant.

461 **Competing Financial Interests**

462 The authors declare no competing financial interests.

463 **Additional Information**

464 None.

465 **References**

¹ Blunt, J. W.; Copp, B. R.; Keyzers, R. A.; Munro, M. H. G.; Prinsep, M. R. *Nat. Prod. Rep.* **2013**, *30*, 237-323.

² (a) Raju, R.; Piggott, A. M.; Conte, M.; Tnimov, Z.; Alexandrov, K.; Capon, R. J. *Chem. Eur. J.* **2010**, *16*, 3194-3200; (b) Raju, R.; Piggott, A. M.; Quezada, M.; Capon, R. J. *Tetrahedron* **2013**, *69*, 692-698.

³ Raju, R.; Piggott, A. M.; Huang, X.-C.; Capon, R. J. *Org. Lett.* **2011**, *13*, 2770-2773.

⁴ Bis, D. M.; Ban, Y. H.; James, E. D.; Alqahtani, N.; Viswanathan, R.; Lane, A. L. *ChemBioChem* **2015**, *16*, 990-997.

⁵ Wang, M.; Feng, X.; Cai, L.; Xu, Z.; Ye, T. *Chem. Comm.* **2012**, *48*, 4344-4346.

⁶ Wang, H.; Reisman, S. E. *Angew. Chem., Int. Ed. Engl.* **2014**, *53*, 6206-6210.

- ⁷ Roettig, M.; Medema, M. H.; Blin, K.; Weber, T.; Rausch, C.; Kohlbacher, O. *Nucleic Acids Res.* **2011**, *39*, W362-W367.
- ⁸ (a) Luk, L. Y. P.; Qian, Q.; Tanner, M. E. *J. Am. Chem. Soc.* **2011**, *133*, 12342-12345; (b) Mahmoodi, N.; Qian, Q.; Luk, L. Y. P.; Tanner, M. E. *Pure Appl. Chem.* **2013**, *85*, 1935-1948; (c) Mahmoodi, N.; Tanner, M. E. *ChemBioChem* **2013**, *14*, 2029-2037.
- ⁹ (a) Li, S.-M. *Phytochemistry* **2009**, *70*, 1746-1757; (b) Yin, W.-B.; Grundmann, A.; Cheng, J.; Li, S.-M. *J. Biol. Chem.* **2009**, *284*, 100-109.
- ¹⁰ Pockrandt, D.; Li, S.-M. *ChemBioChem* **2013**, *14*, 2023-2028.
- ¹¹ Schubert, H. L.; Blumenthal, R. M.; Cheng, X. D. *Trends Biochem. Sci.* **2003**, *28*, 329-335.
- ¹² Giessen, T. W.; von Tesmar, A. M.; Marahiel, M. A. *Biochemistry* **2013**, *52*, 4274-4283.
- ¹³ Belin, P.; Le Du, M. H.; Fielding, A.; Lequin, O.; Jacquet, M.; Charbonnier, J.-B.; Lecoq, A.; Thai, R.; Courcon, M.; Masson, C.; Dugave, C.; Genet, R.; Pernodet, J.-L.; Gondry, M. *Proc. Natl. Acad. Sci. U. S. A.* **2009**, *106*, 7426-7431.
- ¹⁴ M. J. Smanski, J. Casper, R. M. Peterson, Z. Yu, S. R. Rajski and B. Shen, *J. Nat. Prod.* **2012**, *75*, 2158-2167.
- ¹⁵ J. P. Gomez-Escribano and M. J. Bibb, *Microbiol. Biotechnol.* **2011**, *4*, 207-215.
- ¹⁶ James E.; Alqahtani, N.; Viswanathan R.; Lane A. L. *Planta Med.* **2014**, *80*, PJ5.
- ¹⁷ Yang, J. Y.; Sanchez, L. M.; Rath, C. M.; Liu, X.; Boudreau, P. D.; Bruns, N.; Glukhov, E.; Wodtke, A.; de Felicio, R.; Fenner, A.; Wong, W. R.; Linington, R. G.; Zhang, L.; Debonsi, H. M.; Gerwick, W. H.; Dorrestein, P. C. *J. Nat. Prod.* **2013**, *76*, 1686-1699.
- ¹⁸ Nguyen, D. D.; Wu, C.-H.; Moree, W. J.; Lamsa, A.; Medema, M. H.; Zhao, X.; Gavilan, R. G.; Aparicio, M.; Atencio, L.; Jackson, C.; Ballesteros, J.; Sanchez, J.; Watrous, J. D.; Phelan, V. V.; van de Wiel, C.; Kersten, R. D.; Mehnaz, S.; De Mot, R.; Shank, E. A.; Charusanti, P.; Nagarajan, H.; Duggan, B. M.; Moore, B. S.; Bandeira, N.; Palsson, B. O.; Pogliano, K.; Gutierrez, M.; Dorrestein, P. C. *Proc. Natl. Acad. Sci. U. S. A.* **2013**, *110*, E2611-E2620.

- ¹⁹ (a) Repka, L. M.; Ni, J.; Reisman, S. E. *J. Am. Chem. Soc.* **2010**, *132*, 14418-14420; (b) Repka, L. M.; Reisman, S. E. *J. Org. Chem.* **2013**, *78*, 12314-12320.
- ²⁰ Takase, S.; Itoh, Y.; Uchida, I.; Tanaka, H.; Aoki, H. *Tetrahedron* **1986**, *42*, 5887-5894.
- ²¹ Thandavamurthy, K.; Sharma, D.; Porwal, S. K.; Ray, D.; Viswanathan, R. *J. Org. Chem.* **2014**, *79*, 10049-10067.
- ²² (a) Guo, Y.-C.; Cao, S.-X.; Zong, X.-K.; Liao, X.-C.; Zhao, Y.-F. *Spectroscopy*, **2009**, *23*, 131-139; (b) Furtado, N. A. J. C.; Vessecchi, R.; Tomaz, J. C.; Galembeck, S. E.; Bastos, J. K.; Lopes, N. P.; Crotti, A. E. M. *J. Mass Spectrom.* **2007**, *42*, 1279-1286.
- ²³ Micallef, M. L.; Sharma, D.; Bunn, B. M.; Gerwick, L.; Viswanathan, R.; Moffitt, M. C. *BMC Microbiol.* **2014**, *14*, 213.
- ²⁴ (a) Aravind, L.; de Souza, R. F.; Iyer, L. M. *Biology Direct* **2010**, *5*, 48; (b) Bonnefond, L.; Arai, T.; Sakaguchi, Y.; Suzuki, T.; Ishitani, R.; Nureki, O. *Proc. Natl. Acad. Sci. U. S. A.* **2011**, *108*, 3912-3917; (c) Giessen, T. W.; von Tesmar, A. M.; Marahiel, M. A. *Chem. Biol.* **2013**, *20*, 828-838.
- ²⁵ Vetting, M. W.; Hegde, S. S.; Blanchard, J. S. *Nat. Chem. Biol.* **2010**, *6*, 797-799.
- ²⁶ Gondry, M.; Sauguet, L.; Belin, P.; Thai, R.; Amouroux, R.; Tellier, C.; Tophile, K.; Jacquet, M.; Braud, S.; Courcon, M.; Masson, C.; Dubois, S.; Lautru, S.; Lecoq, A.; Hashimoto, S.-I.; Genet, R.; Pernodet, J.-L. *Nat. Chem. Bio.* **2009**, *5*, 414-420.
- ²⁷ Belin, P.; Moutiez, M.; Lautru, S.; Seguin, J.; Pernodet, J.-L.; Gondry, M. *Nat. Prod. Rep.* **2012**, *29*, 961-979.
- ²⁸ Borthwick, A. D. *Chem. Rev.* **2012**, *112*, 3641-3716.